

Table 1 Variation in α_{crit}

Number of terms	α_{crit} (to 2 significant figures)
2	5.5
5	5.6
10	5.7
15	5.8

lem originating from a second-order linear differential equation having homogeneous boundary conditions. Theoretical treatment indicates that a condition for the eigenvalues of such a system to be always real is that the quotient of the coefficients of the second derivative and the " λy " term be positive in the interval.⁴ For Eq. (2) the coefficients are constants and the result follows trivially.

References

- ¹ Keldysh, M. V., "On B. G. Galerkin's method for the solution of boundary value problems," *Izv. Akad. Nauk SSSR, Ser. Mat.* 6, 309-330 (1942); also NASA TT F-195 (1964).
- ² Petrov, G. I., "Application of Galerkin's method to the problem of stability of the flow of a viscous liquid," *Prikl. Mat. Mekh.* 4, 3-12 (1940).
- ³ Bisplinghoff, R. L. and Ashley, H., *Principles of Aeroelasticity* (John Wiley and Sons, Inc., New York, 1962), Chap. 8, p. 426.
- ⁴ Ellen, C. H., "Oblique shock wave interaction with an elastic surface," Ph.D. Thesis, Univ. of Sydney, Sydney, Australia, Appendix 3, p. 71 (1965).

Normal Shock Location of Underexpanded Gas-Particle Jets

ANDREW B. BAUER*

Aeronutronic, Newport Beach, Calif.

Nomenclature

- η = $r/R(x)$
 x = axial distance from the nozzle exit plane
 r = radial distance from axis
 $R(x)$ = radius of the outer edge of the gas cloud or plume
 R_0 = radius of the nozzle exit plane
 v = velocity normal to the axis
 ρ = gas density
 ρ_0 = averaged value of ρ at $x = 0$
 a_0 = sonic speed at $x = 0$
 $B(\gamma) = 1/(\gamma - 1)$
 $D(\gamma)$ = an unknown function

Introduction

AN important consideration in underexpanded rocket nozzle plumes is the location of the normal shock, since the shock structure affects the radiation of the plume. This note makes use of a simple physical model to show how solid particles affect the normal shock location.

The model is based on the assumption that the ambient pressure is much smaller than the jet exit pressure, producing a greatly underexpanded jet. Under these conditions, the effect of the ambient pressure on the flow near the plume axis may be neglected. The flow parameters near the axis are calculated by the analogy between the unsteady expansion of a cylindrical gas cloud and the steady hypersonic flow from a nozzle. Hence, the model applies only to nozzles that have a sufficiently high exit Mach number.

The model also uses the assumption of no particle lag in the supersonic portion of the plume, although it treats both

no-lag and complete-lag flows behind the normal shock. Except for the recognition of particle drag, viscous effects are neglected throughout the analysis.

The normal shock location is based on the method given by Adamson¹ and by Adamson and Nicholls,² since it is simpler to apply than the methods of D'Atorre and Harshbarger³ and Eastman and Radtke.⁴

Expansion of the Rocket Plume

The hypersonic blast or expanding gas-cloud analogy used here has been pointed out both by Mirels and Mullen⁵ and by Greifinger and Cole.⁶ The essential point is that the flow problem parallel to the rocket plume axis may be decoupled mathematically from the flow normal to the axis by neglecting terms of order δ^2 as compared with 1, where δ is a characteristic slope of the plume streamlines. This will be true if the nozzle-exit plane Mach number M_0 is such that $M_0^2 \gg 1$, provided that the gas specific heat ratio γ is not nearly equal to 1. Then, the radial flow problem is just that of the gas cloud.

For the expansion of a cylindrical gas cloud, both Sedov⁷ and Keller⁸ show that, after a long time, a self-similar solution exists in the form of

$$\rho/\rho_0 = D(\gamma)(R_0 M_0/x)^2(1 - \eta^2)^{B(\gamma)} \quad (1)$$

$$v/a_0 = \eta(R_0 M_0/x)(R/R_0) \quad (2)$$

where the dimensionless time t has been replaced by the downstream distance ($x/R_0 M_0$) and where R is given for large values of $x/(M_0 R_0)$ as

$$R(x) = [2^{1/2}/(\gamma - 1)](x/M_0 R_0)R_1 \quad (3)$$

These equations are valid for $R^{2(\gamma-1)}$ large compared to $R_0^{2(\gamma-1)}$; R_1 will be defined later.

At $x = 0$, the rocket nozzle has a density distribution that is, in general, different from $(1 - \eta^2)^{1/(\gamma-1)}$. Hence, the question remains of whether the distribution will tend to approach the form $(1 - \eta^2)^{1/(\gamma-1)}$ for large values of $(x/M_0 R_0)$. Mirels and Mullen⁵ settle the question by equating the mass-flow rate past $x = 0$ to the mass-flow rate at large values of $(x/M_0 R_0)$, and by doing the same for energy-flow rate. They also assume the condition that $R_1 = R_0$, where R_1 is the radius of the self-similar density distribution at $x = 0$ that is equivalent to the real rocket nozzle density distribution at $x = 0$. These three conditions determine the three unknowns $D(\gamma)$, $B(\gamma)$, and R_1 . This leads to $B(\gamma) = 2/(\gamma - 1)$, although $1/(\gamma - 1)$ is the only self-similar exponent that satisfies the equations of motion.^{7,8} Of course, it has not been shown that the plume would be stable in or tend toward the self-similar form, but in the absence of any evidence to the contrary, it will be assumed that the plume approaches this form, so that $B(\gamma) = 1/(\gamma - 1)$. Then we may use the mass and energy conservation equations to calculate $D(\gamma)$ and the ratio (R_1/R_0) .

Mass conservation gives

$$\rho_0 u_0 \pi R_0^2 = R^2 \int_0^1 \rho u_m 2\pi \eta d\eta \quad (4)$$

and energy conservation gives

$$\left(\frac{\rho_0 a_0^2}{\gamma - 1} \right) \pi R_0^2 = R^2 \int_0^1 \rho k^2 \frac{v^2}{2} 2\pi \eta d\eta \quad (5)$$

where u_0 = axial velocity at $x = 0$, u_m = axial velocity at large x , and $k = u_m/u_0$. The distinction between u_0 and u_m is added for the purpose of extending the results to cases where M_0 is not strictly hypersonic, that is, to cases where the gas experiences a small but significant axial acceleration just downstream of the exit plane. This, of course, implies some coupling between the axial and the radial-flow problems, which is neglected here. In Eq. (4), the mass flux at $x = 0$ is equated to the mass flux at large values of $x/R_0 M_0$.

Received October 5, 1964; revision received March 23, 1965. This work was supported under Contract No. NOnr 3907(00).

* Principal Scientist, Fluid Mechanics Department. Member AIAA.

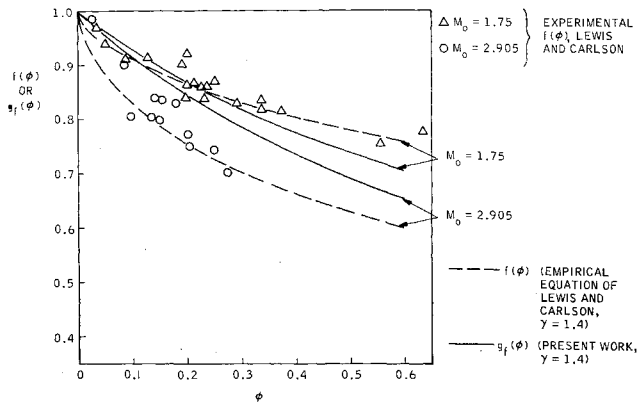


Fig. 1 Normalized shock location distance vs particle mass-flow ratio.

In Eq. (5), the internal energy flux $x = 0$ is equated to the radial-kinetic energy flux at large values of $x/R_0 M_0$, since the internal energy $\rightarrow 0$ as $(x/R_0 M_0) \rightarrow \infty$. These calculations are closely analogous to Eqs. (27a) and (27b) given by Mirels and Mullen.⁵ Insertion of Eqs. (1-3) into Eqs. (4) and (5) leads to

$$D(\gamma) = \gamma(\gamma - 1)/2(2\gamma - 1) \quad (6)$$

$$R_1/R_0 = [(2\gamma - 1)/k]^{1/2} \quad (7)$$

so that

$$\frac{\rho}{\rho_0} = \frac{\gamma(\gamma - 1)}{2(2\gamma - 1)} \left(\frac{M_0 R_0}{x} \right)^2 (1 - \eta^2)^{1/(\gamma - 1)} \quad (8)$$

The preceding was calculated for the plume expansion into a vacuum, but it is assumed to be valid for the present purpose as long as the ambient pressure p_∞ is sufficiently small. This is taken to be $p_0/p_\infty \gg 1$, where p_0 is the stream static pressure at $x = 0$. Then the ambient pressure is not great

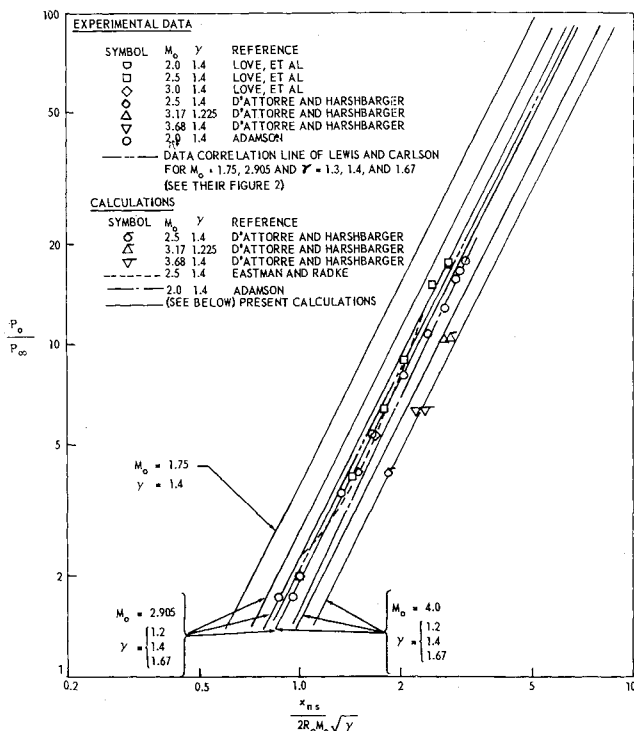


Fig. 2 Ratio of nozzle exit pressure to ambient pressure vs the normal shock-location parameter for zero particle addition.

Table 1 A Comparison of Greifinger's results with the present $D(\gamma)$

γ	$D(\gamma)$	$D_G(\gamma)$
1.11	0.050	0.055
1.2	0.086	0.096
1.4	0.156	0.190
1.67	0.239	0.330

enough to affect the plume density significantly in the region upstream of the normal-shock location.

Greifinger⁹ has numerically solved the axisymmetric hypersonic vacuum-plume equations at large distances from the nozzle and has found that the density is actually a little greater than that given previously. The $D(\gamma)$ given previously compares to Greifinger's result $D_G(\gamma)$ as shown in Table 1.

Particle Addition to the Plume

In general, particle addition to high-speed flows greatly complicates the analysis, as discussed by Hoglund.¹⁰ For sufficiently small particle sizes, such that particle lag is negligible, Hoglund shows that the mixture behaves like a gas with an isentropic exponent λ given by

$$\lambda = \gamma \{ (1 + \varphi C/C_{p0}) / (1 + \gamma \varphi C/C_{p0}) \} \quad (9)$$

where φ is the ratio of particle mass-flow rate to gas mass-flow rate, and C/C_{p0} is the ratio of particle specific heat to gas specific heat at constant pressure.

Normal Shock Location

The hypersonic approximation for the pressure behind a normal shock is,¹¹ for no particle lag,

$$\bar{p}_{ns} = \bar{\rho} \bar{u}_m^2 [2/(\lambda + 1)] \quad (10)$$

where barred symbols will denote the presence of particles in the flow; i.e., $\bar{p} = \rho(1 + \varphi)$, and \bar{u}_m is now the particle and gas velocity just upstream of the shock. This velocity is related to \bar{u}_0 by the isentropic relation¹¹

$$\frac{\bar{u}_m^2}{\bar{u}_0^2} = \frac{\{1 + [(\lambda - 1)/2] \bar{M}_0^2\}}{\{(\bar{M}_0^2/\bar{M}_m^2) + [(\lambda - 1)/2] \bar{M}_m^2\}}$$

where \bar{M}_m is the Mach number just ahead of the shock. Because of the previous requirement that $R^2(\gamma - 1) \gg R_0^2(\gamma - 1)$, one can show that

$$\bar{p}_m/\bar{p}_0 = D(\lambda) (\bar{M}_0 R_0/x_m)^2 \ll 1$$

at $r = \eta = 0$, and, because of the isentropic relation¹¹

$$\frac{\bar{p}_m}{\bar{p}_0} = \left\{ \frac{1 + [(\lambda - 1)/2] \bar{M}_0^2}{1 + [(\lambda - 1)/2] \bar{M}_m^2} \right\}^{1(\lambda - 1)}$$

it is easy to show that

$$\bar{M}_0^2/\bar{M}_m^2 \ll 1$$

which leads to the relation

$$\bar{u}_m/\bar{u}_0 = \{1 + [2/(\lambda - 1)] \bar{M}_0^2\}^{1/2} \quad (11)$$

Then, by using the rule of Adamson and Nicholls² that the normal shock is located such that $\bar{p}_{ns} = p_\infty$, and by using Eqs. (8, 10, and 11), one obtains the shock locations \bar{x}_{ns} as

$$\frac{\bar{x}_{ns}}{R_0} = \left[\frac{\lambda^2(\lambda - 1)}{(\lambda + 1)(2\lambda - 1)} \left(\frac{p_0}{p_\infty} \right) \left(1 + \frac{2}{(\lambda - 1) \bar{M}_0^2} \right) \right]^{1/2} \bar{M}_0^2 \quad (12)$$

The function $g(\varphi)$, which is defined as the ratio of \bar{x}_{ns} to

x_{ns} , where x_{ns} is the shock location without particle addition (but with the same nozzle geometry and exit pressure p_0 used in the calculation of \bar{x}_{ns}), is given by

$$g(\varphi) = \left[\frac{\lambda^2(\lambda - 1)}{(\lambda + 1)(2\lambda - 1)} \frac{(\gamma + 1)(2\gamma - 1)}{\gamma^2(\gamma - 1)} \times \frac{\{1 + [2/(\lambda - 1)\bar{M}_0^2]\}}{\{1 + [2/(\gamma - 1)\bar{M}_0^2]\}} \right]^{1/2} \left(\frac{\bar{M}_0}{\bar{M}_\infty} \right)^2 \quad (13)$$

In some cases, the particles may be sufficiently large so that the flow behind the normal shock may be considered "frozen"; that is, the particles will fail to follow the flow behind the shock. In this event, Eqs. (8, 10, 12, and 13) are replaced by (8f, 10f, 12f, and 13f):

$$\rho/\bar{\rho}_0 = [D(\lambda)/(1 + \varphi)]\bar{M}_0^2(R_0/x)^2 \quad (8f)$$

$$\bar{p}_{nsf} = \rho\bar{u}_m^2(2/\gamma + 1) \quad (10f)$$

$$\left(\frac{\bar{x}_{ns}}{R_0} \right)_f = \left[\frac{\lambda^2(\lambda - 1)\{1 + [2/(\lambda - 1)\bar{M}_0^2]\}}{(\gamma + 1)(2\lambda - 1)(1 + \varphi)} \frac{p_0}{p_\infty} \right]^{1/2} \bar{M}_0^2 \quad (12f)$$

$$g_f(\varphi) = \left[\frac{\lambda^2(\lambda - 1)}{(2\lambda - 1)(1 + \varphi)} \cdot \frac{(2\gamma - 1)}{\gamma^2(\gamma - 1)} \times \frac{\{1 + [2/(\lambda - 1)\bar{M}_0^2]\}}{\{1 + [2/(\gamma - 1)\bar{M}_0^2]\}} \right]^{1/2} \left(\frac{\bar{M}_0}{\bar{M}_\infty} \right)^2 \quad (13f)$$

Results Compared with Experiment

Lewis and Carlson¹² have correlated experimental data showing the change in normal shock location as a function of particle mass-flow ratio φ . Their data are plotted in Fig. 1 in terms of their $f(\varphi)$, which is just the ratio \bar{x}_{ns}/x_{ns} with no qualification as to particle lag conditions. Since it can be argued that the particle lag in these experiments should be important only behind the normal shock, the present $g_f(\varphi)$ is compared to the experimental data in Fig. 1. (The corresponding values of $g(\varphi)$ are larger than $g_f(\varphi)$ but less than 1.)

Since previous equations are applicable to gas-only flows ($\varphi = 0$; $\lambda = \gamma$), Fig. 2 is included to show the comparison between the present calculation and several other calculations and experiments. The data of Love et al. is found in Ref. 13.

References

- Adamson, T. C., Jr., "The structure of the rocket exhaust plume without reaction at various altitudes," The Univ. of Michigan Institute of Science and Technology Rept. 4613-45-T (June 1963).
- Adamson, T. C., Jr. and Nicholls, J. A., "On the structure of jets from highly underexpanded nozzles into still air," J. Aerospace Sci. 26, 16-24 (1959).
- D'Atorre, L. and Harshbarger, F., "Experimental and theoretical studies of underexpanded jets near the mach disc," General Dynamics/Astronautics Rept. GDA-DBE 64-008 (February 19, 1964).
- Eastman, D. W. and Radtke, L. P., "Location of the normal shock wave in the exhaust plume of a jet," AIAA J. 1, 918-919 (1963).
- Mirels, H. and Mullen, J. F., "Expansion of gas clouds and hypersonic jets bounded by a vacuum," AIAA J. 1, 596-602 (1963).
- Greifinger, C. and Cole, J., "One-dimensional expansion of a finite mass of gas into a vacuum," Rand Rept. P 2008 (June 6, 1960).
- Sedov, L. I., *Similarity and Dimensional Methods in Mechanics* (Academic Press Inc., New York, 1959), pp. 271-281.
- Keller, J. B., "Spherical, cylindrical, and one-dimensional gas flows," Quart. Appl. Math. 14, 171-184 (1956).
- Greifinger, C., private communication to R. Foster (February 13, 1963).
- Hoglund, R. F., "Recent advances in gas-particle nozzle flows," ARS J. 32, 662-671 (1962).

¹¹ Liepmann, H. W. and Roshko, A., *Elements of Gasdynamics* (John Wiley and Sons, Inc., New York, 1957), 1st ed., Chap. II, pp. 51, 53, and 59.

¹² Lewis, C. H., Jr. and Carlson, D. J., "Normal shock location in underexpanded gas and gas-particle jets," AIAA J. 2, 776-777 (1964).

¹³ Love, E. S., Grigsby, C. E., Lee, L. P., and Woodling, M. J., "Experimental and theoretical studies of axisymmetric free jets," NASA TR R-6 (1959).

Direct Measurement of Velocity by Hot-Wire Anemometry

ANDREW B. BAUER*

Aeronutronic Applied Research Laboratory,
Newport Beach, Calif.

Introduction

THIS note reports a new method for measuring fluid velocity. The method is of special interest since it can be combined with the standard hot-wire measurement techniques^{1, 2} to determine the fluid pressure p , density ρ , and temperature T , as well as the three velocity components. This is done with a single, small probe.

Standard hot-wire techniques can be used to measure the total temperature T_0 and the product ρU , where U is the velocity component normal to the wire, and where the velocity component parallel to the wire is small as compared with U . Then additional knowledge of the flow, such as constant density conditions or pitot-static tube measurements, will permit U to be determined. The new method determines U independently, so that ρ is calculated easily. The measurement of T_0 then makes it a simple exercise to calculate T and p .

The technique makes use of two hot wires mounted on a simple probe. The wires are held parallel to each other. The velocity direction is determined by heating wire no. 1 and sensing the heated wake with wire no. 2, as illustrated in Fig. 1. This is accomplished most easily by first rotating the entire probe through an angle φ about an axis parallel to the needle supports. When wire no. 2 is normal to the flow, its temperature and resistance will be a minimum. The resistance is sensed by passing a small constant current through the wire and by measuring the wire voltage. Next, wire no. 1 is moved in the \bar{y} direction until its wake is sensed by a temperature rise in wire no. 2. The position of wire no. 2 with respect to wire no. 1 then determines the flow direction.

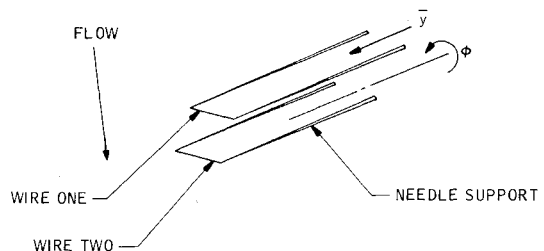


Fig. 1 Probe schematic diagram; a short current pulse heats wire no. 1, which is moved so that its heated wake is sensed by wire no. 2; the relative positions of the two wires and the time for the heat pulse to reach wire no. 2 determine the velocity vector.

Received January 4, 1965; revision received March 17, 1965.

* Principal Scientist, Fluid Mechanics Department. Member AIAA.